Approach to the limits for massive energy and spin deposition into a composite nucleus

D. Jacquet, J. Galin, B. Borderie, D. Gardes, D. Guerreau,* M. Lefort, F. Monnet, M. F. Rivet, and X. Tarrago
Institut de Physique Nucléaire, F-91406, Orsay, Cedex, France

E. Duek† and John M. Alexander
Department of Chemistry, State University of New York at Stony Brook, Stony Brook, New York 11794
(Received 2 April 1985)

We report measurements of correlated fission-like fragments from the reaction 1080 MeV ($E/A=27$ MeV) $^{40}Ar+^{238}U$ and their further correlations with H/He particles. Fusion-like reactions that form highly excited composite nuclei (500–800 MeV) comprise $\approx 40\%$ of the reaction cross section. The probability for such fusion-like reactions is dramatically smaller for ^{40}Ar of E/A of 35–44 MeV. We infer that for this reaction the conditions for high probability of such massive energy and spin containment are near to their limits. The integrated multiplicities for H and He emission are both ≈ 3 for fission reactions that involve 50–100% momentum transfer. These multiplicities are about evenly divided between evaporative and forward-peaked emission; comparison with other results indicates that both have increased by about twentyfold for an increase in projectile energy of 340–1080 MeV. The major sources of evaporative He emission are the very highly excited composite nuclei.

I. INTRODUCTION

Much of our understanding of nuclear reactions at energies of $\lesssim 10$ MeV/nucleon is built around the notion of a mean field (or potential) between the colliding nuclei.[1] The consideration of collective motions (translation, vibration, rotation, etc.) of the nuclei in the context of their mean fields has provided an overall framework in which those essential individual particle movements (excitation, transfers, etc.) have been discussed.[2] By contrast, nuclear reaction phenomena at several GeV/nucleon often seem to be so dominated by nucleon-nucleon collision cascades[3] that even the identification of collective motions requires very special effort.[4] There are many interesting aspects to be studied in the energy range corresponding to the transition between these limiting situations.[5]

One of these is the formation[6,7] and study of massively excited composite nuclei: How much energy and spin can be deposited into a finite nuclear aggregate without essentially instantaneous disintegration?[8–15] Can one determine some of the properties (spin, temperature, moments of inertia, etc.) of such highly excited nuclei?[16–18] The GANIL accelerator[19] is well suited for this quest as it provides heavy projectiles of intermediate energy (e.g., ^{40}Ar of 20–80 MeV/nucleon). Such heavy projectiles can deposit a great deal of energy and angular momentum even for relative nuclear velocities less than the Fermi velocity of the nucleons. For such velocities one might expect that the mean field can maintain most of its control of the collision.

We have chosen the reaction 1080 MeV $^{40}Ar + ^{238}U$ because the excitation energy for complete fusion is very large ($\approx$ 790 MeV) for a relative velocity (27 MeV/nucleon) just below the Fermi velocity. Relatively long-lived composite nuclei can be identified by measurement of the correlated fission fragments.[10] At lower energies this technique has indicated a high probability for complete fusion that gradually yields to incomplete fusion with increasing relative velocity.[10–15,20–24] The decreasing importance of fusion reactions reflects the growing impotence of the nuclear mean field in the face of increasing incident velocity or energy.[10,20,25] The observation of light charged particles, in coincidence with the fission fragments, can provide additional information about all phases of the reaction mechanism.[14–16,22–26] Furthermore, the evaporated light particles can be used to determine properties (spin, moment of inertia, and temperature) of the emitting nuclear aggregates.[16–18,25–28]

Our results indicate that fusion-like reactions for $^{40}Ar + ^{238}U$ comprise $\frac{1}{3}-\frac{1}{2}$ of the reaction cross section at E/A of 27 MeV and give rise to very highly excited ($\approx$500–790 MeV, $\approx 150\hbar$) composite nuclei. On average, there are about three H and three He particles emitted in each fusion-like reaction, roughly evenly divided between evaporative and forward-peaked production. This represents an increase of about twentyfold for an incident energy increase from 340 to 1080 MeV.[26] The final mass of an average fission fragment is about 105 u, and its velocity is close to that inferred from the systematics of fission at much lower energies.[29] In short, the reaction seems to give fission reactions that are very similar to those at low energy, but with a spectrum of deposition energies ranging up to $\approx$790 MeV. As this pattern changes considerably for reactions of Th and U at E/A of 35–44 MeV,[9] we conclude that composite nuclei produced with ^{40}Ar at $E/A=27$ MeV are near to the limit for energy and or spin containment. We also show that evaporative ^4He emission arises primarily from composite nuclei that seem to be quite deformed. A brief sketch of some of this work has been published elsewhere.[25]

II. EXPERIMENTAL TECHNIQUES

The experimental arrangement, as shown in Fig. 1, consisted of three solid-state detectors for fission fragments (F_{1-3}), six three-member solid-state telescopes (T_{1-6}) (all in one plane), and a large position sensitive avalanche detector (PSAD) covering both in-plane and out-of-plane angles. For some measurements the PSAD was moved aft by 20° in order to cover the complete folding-angle distribution for the correlated fission fragments. However, all the measurements involving a light particle in coincidence with fission were performed with the configuration shown in Fig. 1.

A. Fission fragment detection

Fission-like fragments were registered by three high-field, solid state detectors (>60 μm thick) located at 40°, 60°, and 100° with solid angles of 3.77, 5.18, and 5.18 msr, respectively. Both energy and timing signals (start) were generated by these "trigger" detectors. Correlated heavy fragments were recorded in a 20×20 cm^2 position sensitive avalanche detector[30] located ≈30 cm from the target (30° aperture both in and out of plane). The center line of the PSAD was mounted above the detector plane to ensure a wide span for the out-of-plane angles, at least on one side of the reaction plane. Four signals were generated in this detector: an analog signal (related to the energy deposition in the gas), a timing signal, and both horizontal (x) and vertical (y) position signals. The analog signal was used to discriminate fission fragments (relatively high energy loss) from lighter particles of smaller energy loss, and the timing signal indicated that the ratio of random to real coincidence was negligible. Typical efficiencies for the horizontal and vertical position signals were $\approx85\%$ and $\approx65\%$, respectively.

B. Light charged particle detection

The particle telescopes T_{1-4} were located at 15°, 30°, 115°, and 160°, respectively, on the same side as the fission trigger detectors. On the other side T_5 and T_6 were mounted behind the PSAD at $-62°$ and $-39°$, respectively. Solid angles were between 1 and 10 msr. Particle telescopes consisted of three detectors with the following thickness ranges: 50—140 μm, 500—1000 μm, and 4—5 mm. The thinner detectors were used in the backward-angle telescopes. Each telescope was enabled by its second member, and the respective detection thresholds are indicated in the figures which follow. The total Si thickness was not sufficient to stop the H/He particles of highest energies at 15° and 30°. A distinction between H and He was always clear, but energy information was sometimes lost. (Only the unambiguous parts of the energy spectra are shown in Fig. 9.) The multiplicities for He particles are not affected even at high energies by this detector selection. However, the higher energy H particles at 15° and 30° did not deposit enough energy to enable the telescope, and thus were lost.

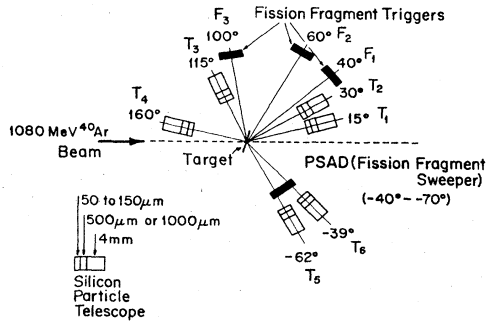

FIG. 1. Experimental arrangement: fission fragment trigger detectors (F_{1-3}) of high-field Si; position-sensitive avalanche detector (PSAD) 20×20 cm^2; and three-member Si particle telescopes (T_{1-6}) (all in plane).

Time-of-flight differences between a fission fragment trigger detector and a light particle telescope were also recorded. Thus, after identification of the light particle, the true time-of-flight for the fission fragment (between target and the trigger detector) could be deduced. By use of energy and time of flight, its mass could also be estimated. The procedure of Kaufman *et al.*[31] was followed to correct for pulse height defect in the fission detector as a function of mass.

The ^{238}U target (320 μg/cm^2 thick) was deposited on an ≈130 μg/cm^2 aluminum backing. A thin aluminum cover layer (25 μg/cm^2) was also evaporated on the other side of the target to give some protection against oxidation. The target ladder was maintained at a positive potential of 25 kV in order to reduce the electron spray onto the detectors. Average beam intensities were ≈10 nA (electrical), and coincidence data were obtained during about 30 h of irradiation.

III. CORRELATIONS BETWEEN THE FISSION-LIKE FRAGMENTS: THE FORMATION PROBABILITY FOR HIGHLY EXCITED COMPOSITE NUCLEI

For many years measurements of fission-fragment angular correlations have been used to gain information concerning momentum and energy transfers from the translational motion of a projectile into momentum and excitation energy of a heavy target-projectile composite nucleus.[32] Several recent papers have discussed the systematic patterns that emerge from these studies.[10—13] The fractional momentum transfer has been found to be primarily a function of one parameter,[10] the relative velocity of the collision partners at impact $[(E_{\rm lab}-V_{\rm lab})/A_{\rm projectile}]^{1/2}$. For Th and U targets that are very fissile, these angular correlation studies have often revealed two distinct peaks or reaction groupings: one at small folding angles corresponding to large momentum transfers (fusion-like fission) and a second at large folding angles corresponding to small momentum transfers (sequential fission after other inelastic transfer reactions). It is important to establish the relative probabilities for these processes in order to gain a view of the reaction mechanism at the time of the primary impact.

In Fig. 2 we show results for the (in-plane) angular correlations of fission-like fragments from reactions of ^{40}Ar with Th and U. Our own results for ^{40}Ar at E/A of 27 MeV [Fig. 2(b)] have been obtained by summing over out-of-plane angles and combining the data from all three trigger detectors. Data from the trigger at 40° (F_1: circle) and 60° (F_2: square) were normalized for overlapping folding angles ($\theta_F \approx 108°$). Data for the trigger at 100° (F_3: triangle and inverted triangle) were obtained from two separate positions of the PSAD and normalized to account for the change in (PSAD) efficiency. The relative intensities for the two peaks have been corrected to the same solid angle, but not for their respective Jacobians.

Our results for ^{40}Ar at E/A of 27 MeV [Fig. 2(b)] and those for E/A of 8.5 MeV (Ref. 26) [Fig. 2(c)] exhibit very prominent peaks for fusion-like reactions. By contrast the results of Pollaco *et al.*[9] for E/A of 44 MeV [Fig. 2(a)] and Leray *et al.*[9] for E/A of 35 MeV indicate that this prominent peak has essentially disappeared. Hence we note that an increase of $\approx$20% in projectile velocity (E/A of 27 to 35—44 MeV) leads to at least a fivefold decrease (if not a loss of identity) for fusion-like processes. The systematic pattern of results from lighter projectiles[10] does not lead one to expect such a reduction for the probability for fusion-like reactions. The heavy projectile ^{40}Ar carries more energy and angular momentum than its smaller siblings, and it is possible that this heavy load rather suddenly exceeds the capacity of the composite nucleus for energy and spin containment. Thus it may be that with 1080 MeV ^{40}Ar we have synthesized fusion-like composite nuclei with lifetime expectancy barely long enough to allow fusion-like decay in high abundance.

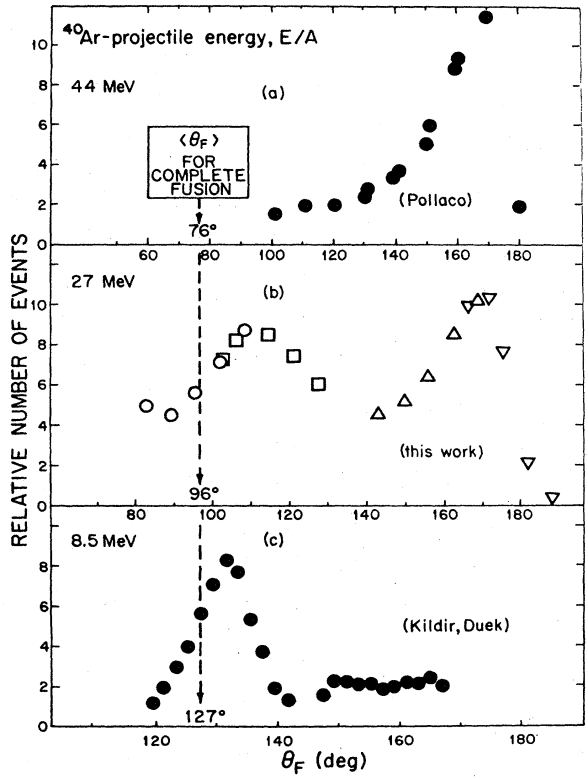

FIG. 2. Number of events versus folding angle θ_F ($\theta_{\text{trigger}} + \theta_{\text{sw}}$ for the two fission fragments): (a) 44 MeV/nucleon ^{40}Ar + Th (Ref. 9); (b) 27 MeV/nucleon ^{40}Ar + U (this work); (c) 8.5 MeV/nucleon ^{40}Ar + U [Ref. 26 and M. Kildir *et al.*, Z. Phys. A **306**, 323 (1982)]. Additional data from the authors of Ref. 9 indicate the absence of a peak for very large momentum transfer. The symbols in (b) are for different trigger angles: 40° ○, 60° □, 100° △ and ▽.

By integrating the number of events under the broad peak at small folding angles we can estimate the cross section for fusion-like reactions (σ_f) and the associated entrance-channel spin zone [zero to $(\sigma_f/\pi\lambda\!\!\!^{-2})^{1/2}$ or l_f within the crude sharp cutoff approximation]. For ^{40}Ar of $E/A = 8.5$ MeV the result is $\sigma_f = 1040$ mb and $l_f = 124\hbar$ (the fission angular distribution here has been found to approach $1/\sin\theta$).[33] For 27 MeV/nucleon we estimate that $\sigma_f = 1.4$—2.3 b (compared to the reaction cross section[34] of 4.7 b) and $l_f = 260\hbar$—$330\hbar$ (the limits result from assuming an isotropic or $1/\sin\theta$ angular distribution.) In both cases the fusion-like reactions comprise about 40% of the reaction cross section. In Sec. VI we will give more consideration to the spin distribution of the composite nuclei that are formed.

One can estimate the range of excitation energies deposited in the composite nucleus after fusion-like collisions by comparing the observed folding-angle distribution to reaction simulation calculations.[20] Such a comparison is shown in Fig. 3. For this calculation we have used the Monte Carlo code LINDA,[35] which required input information concerning the forward-peaked particles emitted during the fast impact that ultimately leads to fusion. From the results of Holub *et al.*[36] we estimate that $\approx$4 forward-peaked neutrons are emitted. Because the thickness of our particle detectors was not sufficient to record the upper part of the energy spectra, we have used the results of Awes *et al.*[24] [from the reaction ^{16}O ($E/A = 20$ MeV) + ^{238}U] to describe the relative abundances and energy spectra of $^{1-3}$H and ^{4}He. Our own results have led us to characterize the angular distributions as exponentially decreasing with c.m. angle with half angles of $\approx$15° for H isotopes and $\approx$10° for He. To fit the simulated curves to the broad fusion-like peak at $90° < \theta_F < 120°$, we have

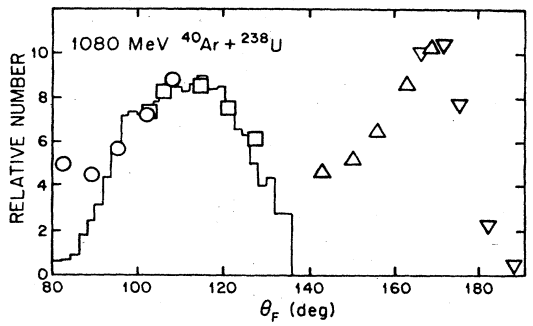

FIG. 3. Comparison of the observed fragment-fragment correlations for fusion-like reactions to a reaction simulation calculation (histogram) as described in the text.

varied the mean number of forward-peaked charged particles (consistent with Table I below) and their standard deviation. (The Gaussian distribution for the number of these direct particles is, of course, truncated at zero, which corresponds to complete fusion.) We have found that a fit to the peak at $\theta_F \approx 110°$ requires on average the emission of ≈ 1.2, 0.4, 0.3, and 1.3^{1-3}H and ^{4}He particles, respectively (forward peaked) and $\approx 25\%$ of essentially complete fusion. A standard deviation about this mean of ≈ 4 particles gives rise to a wide distribution of θ_F for incomplete fusion that merges with that for complete fusion into the one broad peak shown in Fig. 3. The average deposition energy is ≈ 540 MeV, with a wide dispersion ranging up to 790 MeV for complete fusion. In Sec. VI we discuss some aspects of the decay of these massively excited composite nuclei as given by the study of the associated He particles.

A rough estimate has been made of the probability for low momentum transfer by consideration of the peak in Fig. 2(b) at $\theta_F \approx 165°$. We find that the peaks at $\theta_F \approx 110°$ and at 165° reflect rather similar integrated cross sections. In the next section we discuss the general features of H and He emission associated with these two groups.

IV. GENERAL PROPERTIES OF THE H/He PARTICLES EMITTED IN COINCIDENCE WITH THE FISSION-LIKE FRAGMENTS

Most of the light particles emitted in heavy ion reactions between heavy nuclei are neutrons, next are the H/He particles, and finally in quite small abundances are Li, Be, B, etc. Many neutrons are evaporated from either the projectile-like or fission-like fragments,[37–48] and thus, for a time,[37–42] it was relatively difficult to use them as a probe of the composite nuclei. The abundance of charged-particle evaporation from the fully accelerated fragments is much less,[26] and therefore a number of studies have been able to identify both direct and evaporative ^{4}He emission associated with the composite nucleus.[18] The direct particles give information on the mechanism for formation of the composite nucleus;[49] the evaporative particles give information on the emitters, be they the composite nuclei before or near to scission[26] or the newly formed fragments after scission.[50] The first task toward the extraction of such information is the qualitative identification of each class of emission and the estimation of its multiplicity. Such qualitative discussions are the objectives of this section and Sec. VI.

In Fig. 4 we show differential multiplicities $dM/d\Omega$ for H/He production as a function of the folding angle between the pair of coincident fission fragments. There is a distinct difference between the forward-peaked H/He particles and the evaporation-like H/He at backward angles. This latter group is distinctly favored for the fusion-like reactions of small folding angles ($90° < \theta_F < 120°$). The very large deposition energies that characterize these fusion-like collisions seem to provide the driving force for evaporation-like H/He emission. We will return to this point in Sec. VI. The forward-peaked H/He particles arise from the whole range of folding angles, but with a distinct preference for $\theta_F \approx 140°$. It is interesting that $\theta_F \approx 140°$ corresponds to the minimum in the

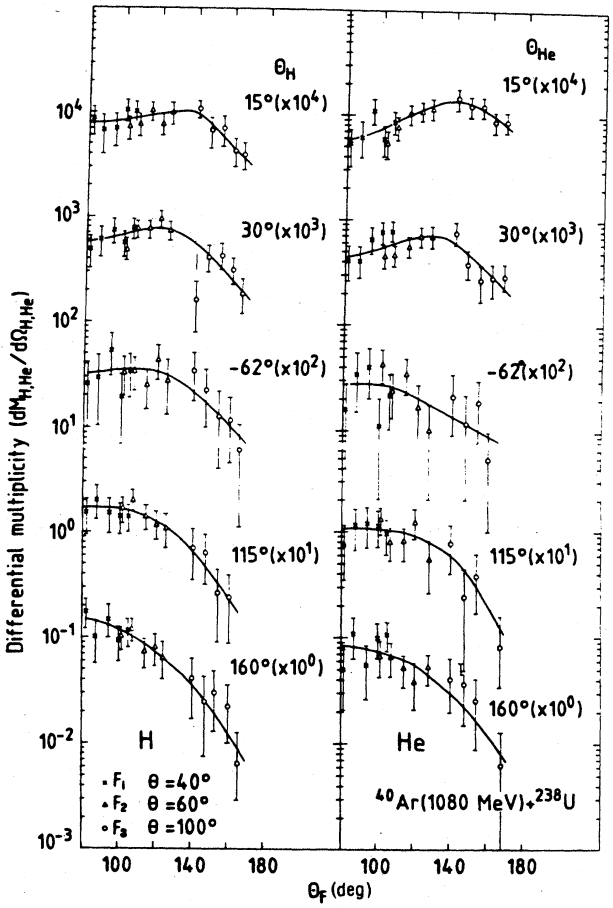

FIG. 4. Differential multiplicities for H/He vs θ_F for various angles $\theta_{H/He}$.

fragment-fragment correlation curve shown in Fig. 2(b). This extensive forward-peaked emission (and its association with $\theta_F \approx 140°$ in Fig. 2) might be an indication of the onset of another process, with intermediate impact parameter, which does not preferentially lead to binary fission.

Angle integrated multiplicities for H and He particles have been obtained by assuming isotropy in the out-of-

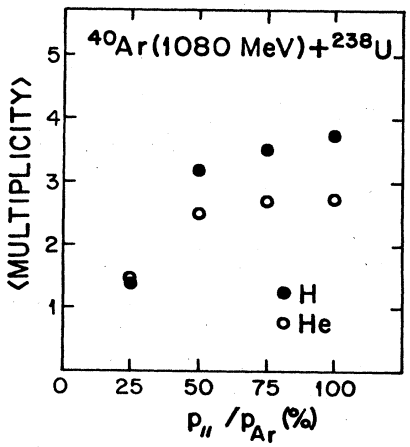

FIG. 5. Angle and energy integrated multiplicities for H/He vs fractional momentum transfer $p_{\parallel}/p_{Ar}$.

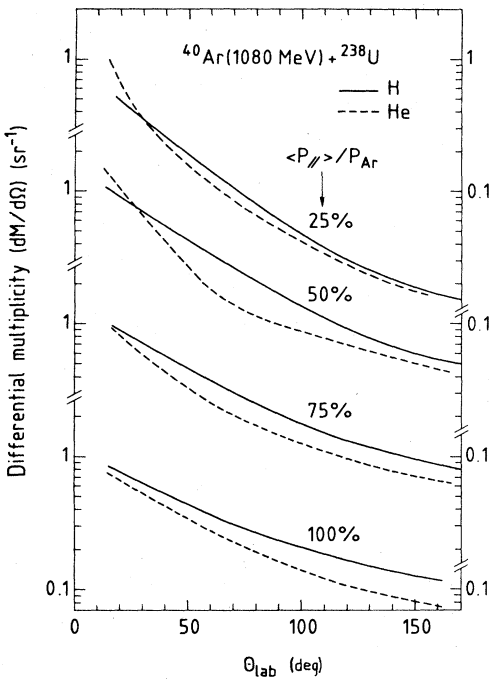

FIG. 6. Differential multiplicities versus laboratory angle for H and He.

plane angle; they are shown in Fig. 5 as a function of the (approximate) fractional momentum transfer ($p_{||}/p_{Ar}$). These angle integrated multiplicities are almost constant at 2.5—4 for momentum transfers of 50—100%, but are considerably smaller for the most peripheral reactions of $p_{||}/p_{Ar} < 25\%$. For these reactions the missing momentum (of $>75\%$) has presumably been carried away by heavier, projectile-like fragments.[51]

From the angular distributions a rough division of these particle multiplicities can be made into evaporative and forward-peaked components. These angular distributions are shown in Fig. 6. Assignment of the backward-angle production has been made to evaporative emission processes that were normalized at 160° and taken to be isotropic in the frame of the appropriate average fissile nucleus. The remaining H/He production is termed the forward-peaked component. Results are summarized in Table I.

The multiplicities for forward-peaked H/He emission have increased by about twentyfold for ^{40}Ar reactions at E/A of 27 MeV compared to those for E/A of 8.5 MeV.[26] This indicates a tremendous increase in the probability of partial or incomplete fusion for the fusion-like reactions of $p_{||}/p_{Ar} > 50\%$. Nevertheless, the mean nuclear field seems to have been effective in catching $\frac{1}{3}-\frac{1}{2}$ of the reactions at E/A of 27 MeV into a fusion-like component. This rapidly increasing trend for the forward-peaked particle spray with increasing incident energy probably continues to E/A of 44 MeV and beyond. If so, it may well be related to the collapse of the fusion-like reaction probability at E/A of 44 MeV as shown in Fig. 2.

TABLE I. Multiplicities[a] for He vs fractional momentum transfer.

M \ $p_{\|\|}/p_{\text{projectile}}$	0.25	0.50	0.75	1.0
Total He	1.46	2.50	2.70	2.75
Evaporative He	0.22	0.70	1.30	1.60
Forward-peaked He	1.24	1.80	1.40	1.15

[a]Standard deviations are about ±20%.

V. AVERAGE VELOCITIES, ENERGIES, AND MASSES OF THE HEAVY FRAGMENTS IN COINCIDENCE WITH He PARTICLES

The results and their discussion so far indicate that the reaction 1080 MeV ^{40}Ar + ^{238}U is very similar to fission-like reactions at lower energies. The major differences seem to lie in the very wide spectrum of energy and momentum transfers, rather than in major qualitative changes in the reaction mechanisms. Both the fast impact processes and the slower fission and evaporative processes seem to reflect a high probability for fusion and to be very similar to reactions at lower energy. If this conclusion is correct, then we have a means for production and study of very highly excited and thermalized nuclear matter ($\approx$500—800 MeV). Further tests of the consistency of this picture can be obtained from the measurements of velocities, energies, and masses of the heavy fragments.

We have determined the velocity, energy, and mass of those fission-like fragments that hit any of the trigger detectors for those events in coincidence with a He particle. The time of flight difference between the fission fragment and the He particle was recorded. The actual time of flight of the fragment could then be deduced by subtracting the time of flight for He (always taken to be ^{4}He). The energy pulse for each fragment was corrected for pulse height defect as a function of mass.[31])

Two types of events were recorded: double coincidences between any telescope and any fission-fragment trigger detector, and triple coincidences for which the avalanche counter also fired. The analysis of the triple coincidences, despite the poor statistics, can be most easily understood, and so we examine them first. We give in Fig. 7(a) the average velocities for fission fragments detected by each of the three trigger detectors (F_1, F_2, and F_3) in coincidence with both the PSAD and one of the light particle telescopes (T_1, T_2, T_4, and T_5). The timing for the telescopes at 115° (T_3) was defective. Only those values are shown for which more than 20 events were recorded.

For these triple coincidence events we see that the average velocity of the fragments depends more on its own detection angle than on the location of the particle telescope. It seems that the folding-angle constraint is most important for fixing the recoil velocity of the fissioning nucleus and hence the average velocity of the fragments. The smaller the folding angle the larger the recoil velocity. This effect is amplified by the fact that the laboratory cross sections for events with larger momentum transfer are also larger at forward angles.

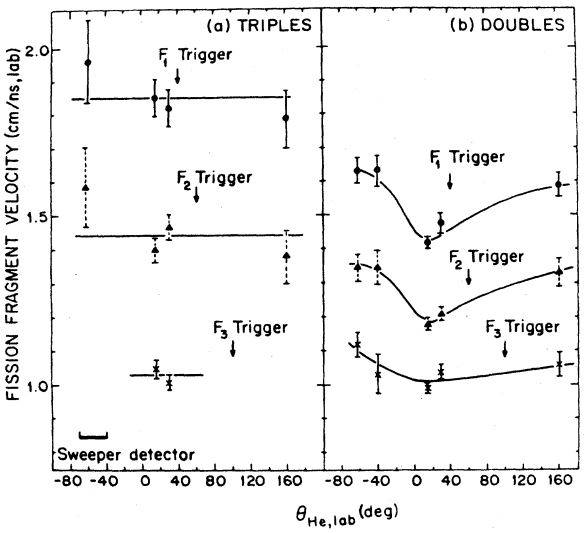

FIG. 7. Average velocities of fission fragments observed in each trigger detector ($F_{1,2,3}$ as indicated) in coincidence with He particles observed at various angles θ_{He}. (a) Triple coincidence required (F_i—PSAD—T_j). (b) Double coincidence required (F_i—T_j).

The same behavior is also clearly evidenced by the energy data shown in Fig. 8(a) which do, in fact, constitute an independent measurement. It is important to note that when both fission fragments are observed in coincidence, the direction of the accompanying ^{4}He particle has very little influence on either the velocity or the kinetic energy of the fission fragments. It seems definite that the folding angle of the coincident fragments puts a strong constraint on the velocity of the fissioning nucleus and hence on that of the resulting fragments.

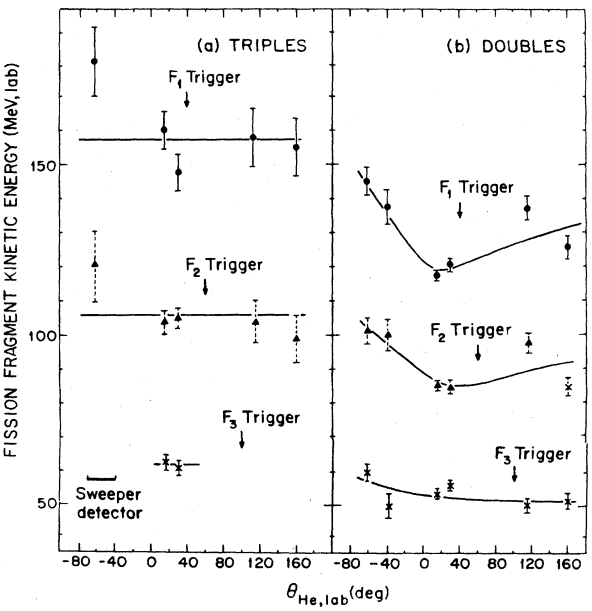

FIG. 8. Same as Fig. 7 but for the average fragment energies. The data points as shown have not been corrected for energy loss in the target (2—7 MeV).

There may be a small exception to this statement for the ^{4}He detector located at $-62°$ (T_5) just behind the PSAD where one fragment was detected. Both the energies and the velocities of the complementary fragment (detected by F_1, F_2, and F_3) seem to be systematically larger for ^{4}He in coincidence with these detectors. A possible explanation for this difference can be found in the properties of those ^{4}He particles emitted by the fragments. Consider the kinematic focusing effect for the emitted He particles if the emitting fission fragments are found essentially in the same direction; in these cases those fragments that emit more ^{4}He would be favored in the PSAD. If the heavy fragments emit more ^{4}He particles (due to their larger excitation energies), then the complementary light fragments would be dominant in the associated trigger detector. This effect could give slightly larger velocities and kinetic energies for fragments in coincidence with T_5. In any event, this effect is fairly small.

Let us now consider the average velocity [Fig. 7(b)] and energy [Fig. 8(b)] of the fission fragments in double coincidence (i.e., those associated with a ^{4}He particle but without any coincidence requirement on the complementary fission fragment). Two clear differences arise in comparison to the data for triple coincidences. For both F_1 and F_2 triggers, the average velocities and energies are smaller for double coincidences, whereas they remain about the same for the F_3 trigger. These effects can be understood qualitatively as follows. At 100° (the F_3 trigger), fragments from high momentum transfers essentially cannot be registered due to the high c.m. velocity which focuses them in the forward direction; only fragments following small momentum transfers can be seen. Therefore, since the requirement of a triple coincidence with the sweeper at $\langle\theta_{sw}\rangle=55°$ also calls for small momentum transfer, it does not bring any strong additional constraint. This is definitely not the situation for double coincidences with F_1 at 40°; at this angle any momentum transfer, large or small, can contribute to the observed fission fragments. It is mainly the requirement for a coincident fragment at a small folding angle (triple coincidence) that has made the selection for large momentum transfers and correspondingly high fragment energies and velocities. Without this constraint (double coincidence) the observed velocities and energies for F_1 result from averages that reflect the distribution of all possible momentum transfers. Hence the results from double coincidence allow the intrusion of more low-momentum transfers and thus lower velocities and energies for the fragments. The situation for F_2 is similar to that for F_1, but differences between triples and doubles for F_2 are less dramatic than for F_1. The highest momentum transfers are not selected in triples for F_2 (only about eighty percent of full momentum transfer).

There is another important effect which shows up in the velocities of the fragments detected at 40° or 60° (F_1 and F_2), but specifically in coincidence with forward emitted ^{4}He particles at 15° or 30°. These fragments have much lower velocities than those associated with particles emitted at more backward angles. As shown in Fig. 4, the ^{4}He particles detected at either 15° or 30° exhibit a large multiplicity for intermediate and low momentum

TABLE II. Average masses (u) for fragments observed in trigger detector F_i in coincidence with He particles recorded in telescope T_j.

		T_1	T_2	T_4	T_5	Average
F_1	triples	99	97	99	98	98±7
	doubles	121	114	104	112	
F_2	triples	113	103	110	99	106±5
	doubles	126	120	103	115	
F_3	triples	115	112			113.5±6
	doubles	115	106	92	97	

transfers. It is precisely this multiplicity effect which shows up here. Since intermediate and small momentum transfers are mainly associated with the forward-peaked particles, the coincident fission fragments (doubles) have received on average only a modest boost from their emitter's velocity. Hence this represents another type of selectivity on the momentum transfer that is given by the associated light particles and not by the emission angle of the correlated fragments.

Let us now consider the average masses, both in the triples and doubles modes, for the different combinations of detectors. A summary of all the results is given in Table II. It is shown in Figs. 7(a) and 8(a) that the statistical errors are large for the triples mode and do not allow us to distinguish any variations of mass with the position of the ^{4}He telescope. Thus the values have been averaged over the following measurements: $\langle M\rangle_{40°}$ (coincidences with T_1, T_2, T_4, T_5)=98±7; $\langle M\rangle_{60°}$ (coincidences with T_1, T_2, T_4, T_5)=106±5; $\langle M\rangle_{100°}$ (coincidences with T_1, T_2)=113.5±6. Experimental uncertainties are discussed in the Appendix.

Masses have not been determined for the fragments that strike the PSAD, but it is possible to deduce them for cases where the trigger and sweeper detectors are nearly symmetric with respect to the beam. This is the case for $F_2=60°$, $\theta_{sw}=40°-70°$ and for $F_1=40°$, $\theta_{sw}=40°-70°$. For these cases the sum of the two fragment masses is twice that for one fragment. This inference cannot be made for the asymmetric trigger angle set at 100° (F_3) for $\langle\theta_{sw}\rangle=55°$; due to the Jacobians the trigger detector is biased toward the light fragments and the sweeper toward the heavy fragment. Therefore, by doubling the value of $\langle M\rangle_{100°}$ we obtain a lower limit for $\langle M_1+M_2\rangle_{100°,55°}$. In sum we find the following values: $\langle M_1+M_2\rangle_{40°,55°}=196\pm14$; $\langle M_1+M_2\rangle_{60°,55°}=212\pm10$; $\langle M_1+M_2\rangle_{100°,55°}>227\pm12$ u.

Can we understand these values in the framework discussed above? For nearly full momentum transfer (F_1) the excitation energy of a compound nucleus would be ≈790 MeV. For symmetric fission, one can estimate a Q value of about 300 MeV,[52] and total kinetic energy for the fragments of 220 MeV which leaves about 870 MeV available for particle emission. Exclusive evaporation of nucleons (neutrons and protons) from the fragments would lead to a lower limit for the number of removed nucleons. If evaporation begins with a temperature of 5 MeV, each nucleon of the evaporation chain would remove on average ≈15 MeV. A similar value of ≈15 MeV has been deduced from the experimental results of Pollaco *et al.*[9] for 44 MeV/nucleon ^{40}Ar + Th. Thus at most (870/15) or 58 nucleons could evaporate from the fission fragments, leading to a total final mass of about 220. The final mass of 197±14 that we have derived from the observations for F_1 seems to be somewhat too small. A rough calculation can also be made for F_2 by assuming that on average both the excitation energy and the transferred momentum are ≈80% of that for full momentum transfer. This estimate gives a total final mass of the fragments of 223 as compared to the observed value 212±11. The emission of composite particles either before or after fission can modify the estimates above. Indeed, on average a composite particle (e.g., ^{4}He) does remove less energy than do the nucleons separately. However, since the number of ^{4}He particles emitted is only about three per reaction, this would not seem to be a major source of additional mass loss.

In summary, we can understand, in a qualitative way, the patterns of the mean fragment velocities and energies shown in Figs. 7 and 8. The wide spectrum of velocity transfers to the fissile composite nucleus is biased in various ways by the different coincidence constraints. The absolute mass values are not completely accounted for, but they are more subject to systematic errors than are the observed trends shown in Figs. 7 or 8 for either the velocities or the energies.

VI. ENERGY SPECTRA FOR THE He PARTICLES: TESTS FOR EVAPORATIVE EMISSION FROM EITHER THE COMPOSITE NUCLEUS OR THE FULLY ACCELERATED FRAGMENTS

For fission-like reactions, induced by projectiles of lower energy, the H/He emission has been found to arise from several different mechanisms. Forward-peaked particles have been attributed primarily to direct ejection at impact but also to sequential evaporation from projectile-like fragments. The less energetic particles (especially at backward angles) have been assigned to evaporation-like processes, partly from the composite nucleus prior to scission and partly from the fully accelerated fission fragments. A much smaller part has been recognized as near-scission emission.[26] The best understood of these processes is that of evaporation: The basic angular symmetry is well known;[53] empirical evaporation barriers have been systematically evaluated from compound-nucleus reactions;[17] nuclear temperatures can be estimated from the measured average momentum transfers and Q values.[52] Therefore the analysis of H/He spectra is usual-

ly begun by a comparison to calculated particle spectra from an evaporation reaction simulation.

In this study we use the Monte Carlo simulation code GANES that has been described elsewhere.[26,54] The program input requires a description of the energy, mass, velocity, and angular momentum distributions for the entrance channels, and the mean energy loss (by particle emission) prior to He evaporation. Then it constructs the intrinsic velocities for evaporative emission and adds them to the velocities of the emitters. We have measured the spectra for He in triple coincidence with two fission-like fragments. Therefore we have calculated evaporation spectra for emission from these fully accelerated fragments as well as for emission from the composite nuclei. These spectra along with detector geometry and velocity diagrams are shown in Fig. 9. In order to improve the statistical significance, we have summed the events triggered by both F_1 and F_2. For the velocity diagrams we show mean velocities from F_1 alone, but the smooth curves from the simulations contain sums for F_1 and F_2 constructed in the same way as the experimental histograms.

The major constraints for the abundance of fragment evaporation (FE, short-dashed line) and composite eva-

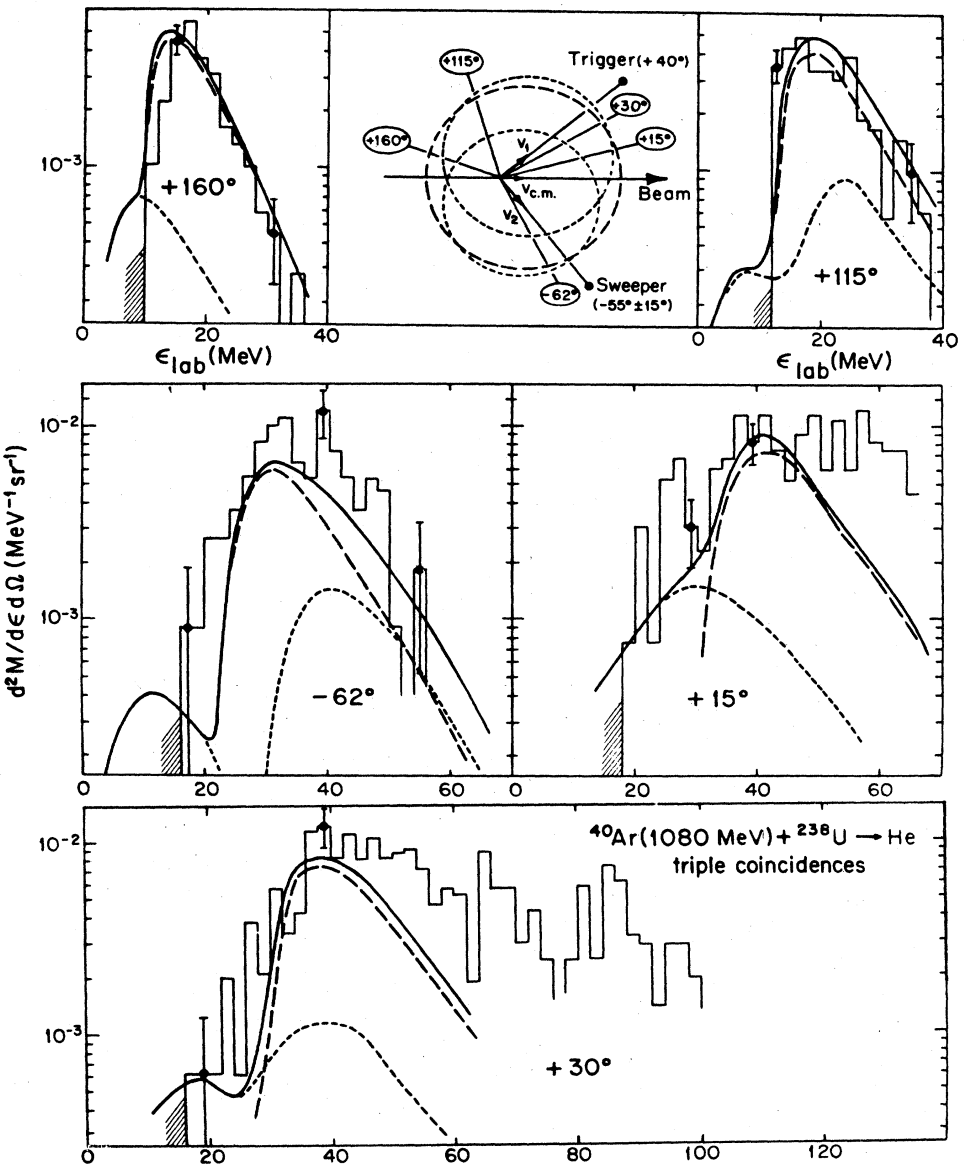

FIG. 9. Energy spectra for He in triple coincidence with a trigger fragment at 40° or 60° and a sweeper fragment in the PSAD. Smooth curves are from simulation for evaporation from fully accelerated fragments(---), from the composite nucleus (— — —), and their sum (——). The telescope angles are shown in relation to an average vector diagram for the F_1 trigger at 40°. The c.m. velocity is indicated as $V_{c.m.}$, the two fission-fragment velocities as V_1 and V_2, and the circles show loci of mean evaporation velocities from the fragments (---) and the composite nuclei (— — —).

poration (CE, long-dashed line) are provided by telescopes T_3 and T_4 at 115° and 160°, respectively. As indicated in the vector diagram, the FE is expected to give the larger mean velocity at 115°, while CE is expected to give the larger velocity at 160°. Therefore, any attempt to account for the spectra at these two angles will be particularly sensitive to the relative amount of CE and FE. As the large peak at ≈ 15 MeV for T_4 at 160° cannot be attributed to FE, it is primarily assigned to CE. Once the abundance of CE is normalized at 160°, its magnitude and shape at all other angles follows from the basic symmetry for evaporation theory. As the spins of all emitters are expected to be essentially perpendicular to the reaction plane, one expects isotropic particle emission in this plane. The CE process also accounts for the bulk of the He spectra at 115°, where FE is most favored kinematically. This leaves room for a maximum contribution (to the He spectra at backward angles) of only $\approx 25\%$ from fragment evaporation.

Another interesting feature of this analysis is the shape of the spectrum from composite nucleus evaporation. For spherical composite nuclei with $J_{\rm rms} \gtrsim 80$, a long, high-energy tail is predicted (similar to that which would be generated by a very high-temperature emitter). The origin of this high energy tail is the spin-off energy from very large exit channel l waves that would be favored from such very high spin spherical nuclei. This high-energy tail is not observed in the data, and we feel that this gives a significant constraint on the properties of the emitting composite nuclei.[54–56] Clearly the angular momentum deposited in those composite nuclei is less than that for the entrance channel l waves due to the emission of particles in the forward-peaked spray. We can estimate the values of $J_{\rm rms}$ for the composite nuclei by assuming that (1) the entrance channel l values increase with decreasing θ_F and (2) that the spin deposition for each value is proportional to $p_{||}/p_{\rm Ar}$ for each value of θ_F. Such a rough estimate leads to $J_{\rm rms} \approx 150\hbar$, and gives simulated He spectra that, for spherical nuclei, are incompatible with the data. However, if the emitting nuclei are deformed into near-prolate shapes of principal axis ratio of > 1.5, then the predicted spectral shapes are acceptable.[54] At this time it is not possible to pursue this point further due to statistical limitations on the data. However, a second experiment is now expected that we hope can provide more detailed constraints on the properties of these very hot and rapidly spinning nuclei.

VII. SUMMARY

We have presented an initial survey of the reaction ^{40}Ar ($E/A = 27$ MeV) + ^{238}U. Fission fragment angular correlation measurements show that $\approx 40\%$ of the reaction cross section goes into fusion-like events. By contrast, other studies[9] have shown that the probability for fusion-like reactions is much smaller for ^{40}Ar of E/A of 35–44 MeV. Such a decrease is not expected from the systematics of fission-fragment angular correlation studies with lighter projectiles.[10] We infer that the reaction 1080 MeV ^{40}Ar + ^{238}U must be producing target-projectile composite nuclei with lifetime expectancy barely long enough to allow fission-like decay in high abundance. By comparison to reaction simulation calculations, we infer that there is a broad spectrum of complete and incomplete fusion reactions with energy depositions ranging from ≈ 500–790 MeV and with $J_{\rm rms} \approx 150\hbar$.

Light H and He particles have been observed in double and triple coincidence with the fission-like products. Integrated multiplicities are greater than three H and approximately equal to three He particles per fusion-like reaction. These values represent an increase of about twentyfold for an incident energy increase from 340 to 1080 MeV [an increase of ≈ 6 in $(E-V)/A$].[26] They are roughly evenly divided between forward-peaked and evaporative emission. The evaporative emission of He is predominantly due to the composite nuclei prior to scission; therefore they offer a probe for further study of the properties of these massively excited and very interesting nuclei.

ACKNOWLEDGMENTS

This experiment was performed at the GANIL national facility at Caen, France. Kind hospitality at GANIL and Orsay is acknowledged by E. D. and J. M. A. as well as that at Stony Brook by D. J. and J. G. We want to thank H. Gauvin, who supervised the realization of the PSAD. The efforts of the GANIL staff are greatly appreciated.

APPENDIX: EXPERIMENTAL UNCERTAINTIES ON THE DETERMINATION OF THE FISSION FRAGMENT MASSES

For a given fission-fragment detector there is an absolute uncertainty on the energy measurement which is expected to be less than $\pm 3\%$ (after pulse height defect corrections). In addition, for F_1 (40°) it is possible that the depletion thickness was insufficient to record the full energy of the lightest fragments of longest range. Therefore, the average mass deduced for F_1 could be low by a small amount. Uncertainties for the fission fragment velocities are estimated to be between 2% and 5%. This rather high value comes from the fact that the actual flight time of a fragment results from the difference between two quantities: (1) the directly measured time difference between the instants the light particle and the fission fragment hit their respective detectors, and (2) the time of flight of the He particle, as determined from its energy and the assumed mass of 4 u. Actually, about 15% of the events, which were analyzed as coincidences between fission fragments and alpha particles, were, in fact, coincidences between fission fragments and ^{3}He. The effect of this error on the fission fragment mass depends on the relative importance of the particle time of flight as compared to the fission fragment time of flight. This error has to be combined with the intrinsic resolution of the timing (which can be estimated at 350 ps) and with the energy resolution.

Taking into account the average over the four different velocity measurements, one finds the following uncertainties:

$$(\Delta M/M)_{40°} = 6.7\%,\ (\Delta M/M)_{60°} = 4.4\%\ ,$$

$$(\Delta M/M)_{100°} = 5\%\ .$$

*Present address: GANIL, B.P. 5027, 14021 Caen, Cedex, France.
†Present address: Department of Chemistry, Brookhaven National Laboratory, Upton, NY 11973.

[1]R. Bass, *Nuclear Reactions with Heavy Ions* (Springer, Heidelberg, 1980).
[2]A. Bohr and B. Mottelson, *Nuclear Structure* (Benjamin, New York, 1975).
[3]Y. Yariv and Z. Fraenkel, Phys. Rev. C **20**, 2227 (1979).
[4]H. A. Gustafsson, H. H. Gutbrod, B. Kolb, H. Lohner, B. Ludewigt, A. M. Poskanzer, T. Renner, H. Riedesel, H. G. Ritter, A. Warwick, F. Weik, and H. Weiman, Phys. Rev. Lett. **52**, 1590 (1984).
[5]D. K. Scott, Nucl. Phys. **A354**, 375c (1981).
[6]M. Lefort, *Heavy Ion Collisions*, edited by R. Bock (North-Holland, Amsterdam, 1980), Chap. 2:46.
[7]J. R. Birkelund and J. R. Huizenga, Annu. Rev. Nucl. Part. Sci. **33**, 265 (1983).
[8]B. Borderie, M. F. Rivet, C. Cabot, D. Fabris, D. Gardes, H. Gauvin, F. Hanappe, and J. Peter, Z. Phys. A **316**, 243 (1984).
[9]E. C. Pollaco, M. Conjeaud, S. Harar, C. Volant, Y. Cassagnou, R. Dayras, R. Legrain, M. S. Nguyen, H. Oeschler, and F. Saint-Laurent, Phys. Lett. **146B**, 29 (1984); see also results for ^{40}Ar (E/A=35 MeV) + ^{238}U from S. Leray *et al.*, Z. Phys. A **320**, 533 (1985).
[10]V. E. Viola, Jr., B. B. Back, K.L. Wolf, T. C. Awes, C. K. Gelbke, and H. Breuer, Phys. Rev. C **26**, 178 (1982), and references therein.
[11]J. Galin, H. Oeschler, S. Song, B. Borderie, M. F. Rivet, I. Forest, R. Bimbot, D. Gardes, B. Gatty, H. Guillemot, M. Lefort, B. Tamain, and X. Tarrago, Phys. Rev. Lett. **48**, 1787 (1982).
[12]G. La Rana, G. Nebbia, E. Tomasi, C. Ngo, X. S. Chen, S. Leray, P. Lhenoret, R. Lucas, C. Mazur, M. Ribrag, C. Cerruti, S. Chiodelli, A. Demeyer, D. Guinet, J. L. Charvet, M. Morjean, A. Peghair, Y. Pranal, L. Sinopoli, J. Uzureau, and R. de Swiniarski, Nucl. Phys. **A407**, 233 (1983).
[13]M. B. Tsang, D. R. Klesch, C. B. Chitwood, D. J. Fields, C. K. Gelbke, W. G. Lynch, H. Utsunomiya, K. Kwiatkowski, V. E. Viola, Jr., and M. Fatyga, Phys. Lett. **134B**, 169 (1984).
[14]S. Song, M. F. Rivert, R. Bimbot, B. Borderie, I. Forest, J. Galin, D. Gardés, B. Gatty, M. Lefort, H. Oeschler, B. Tamain, and X. Tarrago, Phys. Lett. **130B**, 14 (1983).
[15]M. F. Rivet, B. Gatty, H. Guillemot, B. Borderie, R. Bimbot, I. Forest, J. Galin, D. Gardés, D. Guerreau, M. Lefort, X. Tarrago, B. Tamain, and L. Novicki, Z. Phys. A **307**, 365 (1982).
[16]M. F. Rivet, D. Logan, J. M. Alexander, D. Guerreau, E. Duek, M. S. Zisman, and M. Kaplan, Phys. Rev. C **25**, 2430 (1982).
[17]J. M. Alexander, D. Guerreau, and L. C. Vaz, Z. Phys. A **305**, 313 (1982).
[18]L. C. Vaz, D. Logan, E. Duek, J. M. Alexander, M. F. Rivet, M. S. Zisman, Morton Kaplan, and J. W. Ball, Z. Phys. A **315**, 169 (1984), and references therein.
[19]A. Joubert and the GANIL Group, Status Report on the GANIL facility, GANIL Internal Report A-84-04, 1984.
[20]E. Duek, L. Kowalski, M. Rajagopalan, J. M. Alexander, D. Logan, M. S. Zisman, and Morton Kaplan, Z. Phys. A **307**, 221 (1982).
[21]E. Duek, L. Kowalski, M. Rajagopalan, J. M. Alexander, T. W. Debiak, D. Logan, M. Kaplan, M. Zisman, and Y. LeBeyec, Z. Phys. A **307**, 237 (1982).
[22]J. L. Laville, C. Le Brun, J. F. Lecolley, F. Lefebvres, M. Louvel, R. Regimbart, J. C. Steckmeyer, N. Jabbri, R. Bertholet, C. Guet, D. Heuer, M. Maurel, H. Nifenecker, C. Ristori, F. Schlussler, F. Guilbault, and C. Lebrun, Phys. Lett. **138B**, 35 (1984).
[23]B. B. Back, K. L. Wolf, A. C. Mignerey, C. K. Gelbke, T. C. Awes, H. Breuer, V. E. Viola, Jr., and P. Dyer, Phys. Rev. C **22**, 1927 (1980).
[24]T. C. Awes, G. Poggi, C. K. Gelbke, B. B. Back, B. G. Glagola, H. Breuer, and V. E. Viola, Jr., Phys. Rev. C **24**, 89 (1981).
[25]D. Jacquet, E. Duek, J. M. Alexander, B. Borderie, J. Galin, D. Gardés, D. Guerreau, M. Lefort, F. Monnet, M. F. Rivet, and X. Tarrago, Phys. Rev. Lett. **53**, 2226 (1984); M. F. Rivet and B. Borderie, in Tsukuba International Symposium on Heavy Ion Fusion Reactions, Tsukuba, Japan, 1984.
[26]E. Duek, N. N. Ajitanand, J. M. Alexander, D. Logan, M. Kildir, L. Kowalski, Louis C. Vaz, D. Guerreau, M. S. Zisman, Morton Kaplan, and D. J. Moses, Z. Phys. A **317**, 83 (1984).
[27]D. J. Moses, M. Kaplan, J. M. Alexander, D. Logan, M. Kildir, L. C. Vaz, N. N. Ajitanand, E. Duek, and M. S. Zisman, Z. Phys. A **320**, 229 (1985).
[28]Louis C. Vaz and John M. Alexander, Z. Phys. A **318**, 231 (1984).
[29]V. E. Viola, Jr., Nucl. Data **1**, 391 (1966).
[30]D. Gardés and P. Volkov, Orsay Report IPNO-RC-81-08, 1984.
[31]S. B. Kaufman, E. P. Steinberg, B. D. Wilkins, J. Unik, A. J. Gorski, and M. J. Fluss, Nucl. Instrum. Methods **115**, 47 (1974).
[32]V. I. Ostroumov, Dokl. Adad. Nauk SSSR **103**, 409 (1955); W. J. Nicholson and I. Halpern, Phys. Rev. **116**, 175 (1959); T. Sikkeland, E. L. Haines, and V. E. Viola, Jr., Phys. Rev. **125**, 1350 (1962).
[33]K. T. Lesko, S. Gil, A. Lazzarini, V. Metag, A. G. Seamster, and R. Vandenbosch, Phys. Rev. C **27**, 2999 (1983).
[34]W. W. Wilcke, J. R. Birkelund, H. J. Wollersheim, A. D. Hoover, J. R. Huizenga, W. U. Schroder, and L. E. Tubbs, At. Data Nucl. Data Tables **25**, 389 (1980).
[35]E. Duek, L. Kowalski, and J. M. Alexander, Comput. Phys. Commun. **34** 395, 1985.
[36]E. Holub, D. Hilscher, G. Ingold, U. Jahnke, H. Orf, and H. Rossner, Phys. Rev. C **28**, 252 (1983).
[37]B. Tamain, R. Chechik, H. Fuchs, F. Hanappe, M. Morjean, C. Ngô, J. Peter, M. Dakowski, B. Lucas, C. Mazur, M. Ribrag, and C. Signarbieux, Nucl. Phys. **A330**, 253 (1979).
[38]D. Hilscher, J. R. Birkelund, A. D. Hoover, W. U. Schroder, W. W. Wilcke, J. R. Huizenga, A. C. Mignerey, K. L. Wolf, H. F. Breuer, and V. E. Viola, Jr., Phys. Rev. C **20**, 576 (1979).
[39]Y. Eyal, A. Gavron, I. Tserruya, Z. Fraenkel, Y. Eisen, S. Wald, R. Bass, C. R. Gould, G. Kreyling, R. Renfordt, K. Stelzer, R. Zitzmann, A. Gobbi, U. Lynen, H. Stelzer, I. Rode, and R. Bock, Phys. Rev. C **21**, 1377 (1980).
[40]C. R. Gould, R. Bass, J. V. Czarnecki, V. Hartmann, K. Stelzer, R. Zitzmann, and Y. Eyal, Z. Phys. A **294**, 323 (1980).
[41]M. Dakowski, R. Chechik, H. Fuchs, F. Hanappe, B. Lucas, C. Mazur, M. Morjean, J. Peter, M. Ribrag, C. Signarbieux, and B. Tamain, Z. Phys. A **294**, 289 (1980).
[42]A. Gavron, J. R. Beene, B. Cheynis, R.L. Ferguson, F. E. Obenshain, F. Plasil, G. R. Young, G. A. Petitt, M. Jaaskelainen, D. G. Sarantites, and C. F. Maguire, Phys. Rev. Lett. **47**, 1255 (1981).
[43]A. Gavron, J. R. Beene, B. Cheynis, R. L. Ferguson, F. E.

Obenshain, F. Plasil, G. R. Young, G. A. Petitt, M. Jaaskelainen, D. G. Sarantites, and C. F. Maguire, Phys. Rev. Lett. **48**, 835 (1982).

[44]I. Tserruya, A. Breskin, R. Chechik, Z. Fraenkel, S. Wald, N. Zwang, R. Bock, M. Dakowski, A Gobbi, H. Sann, R. Bass, G. Kreyling, R. Renfordt, K. Stelzer, and U. Arlt, Phys. Rev. C **26**, 2509 (1982).

[45]E. Holub, M. Korolija, and N. Cindro, Z. Phys. A **314**, 347 (1983).

[46]Y. Chan, M. Murphy, R. G. Stokstad, I. Tserruya, S. Wald, and A. Budzanowski, Phys. Rev. C **27**, 447 (1983).

[47]A. Gavron, J. R. Beene, B. Cheynis, R. L. Ferguson, F. E. Obenshain, F. Plasil, G. R. Young, G. A. Petitt, C. F. Maguire, D. G. Sarantites, M. Jaaskelainen, and K. Geoffroy-Young, Phys. Rev. C **27**, 450 (1983).

[48]W. Kühn, P. Chowdhury, R. V. F. Janssens, T. L. Khoo, F. Haas, J. Kasagi, and R. M. Ronningen, Phys. Rev. Lett. **51**, 1858 (1983).

[49]M. Blann, Annu. Rev. Nucl. Sci. **25**, 123 (1975).

[50]G.-Y. Fan, H. Ho, P. L. Gonthier, W. Kühn, A. Pfoh, L. Schad, R. Wolski, J. P. Wurm, J. C. Adloff, D. Disdier, V. Rauch, and F. Scheibling, Z. Phys. A **310**, 269 (1983).

[51]V. Borrel, D. Guerreau, J. Galin, B. Gatty, D. Jacquet, and X. Tarrago, Z. Phys. A **314**, 191 (1983).

[52]W. D. Myers and W. J. Swiatecki, Ark. Fys. **36**, 343 (1967).

[53]T. Ericson, Adv. Phys. **9**, 423 (1960); T. Ericson and V. Strutinski, Nucl. Phys. **8**, 284 (1958).

[54]N. N. Ajitanand, R. Lacey, G. F. Peaslee, E. Duek, and J. M. Alexander, submitted to Nucl. Instrum. Methods.

[55]R. Lacey, G. F. Peaslee, H. Delagrange, E. Duek, D. Guerreau, J. M. Alexander, N. N. Ajitanand, L. C. Vaz, L. Kowalski, D. Logan, M. Kildir, M. Kaplan, D. J. Moses, and M. S. Zisman (unpublished).

[56]X. S. Chen, C. Ngô, E. Tomasi, M. Barranco, X. Vinas, and H. Ngô, Nucl. Phys. **A401**, 143 (1983).